
GENERATING SYNTHETIC DATA FOR NEURAL OPERATORS

Erisa Hasani *
Department of Mathematics
University of Texas at Austin
ehasani@utexas.edu

Rachel A. Ward
Department of Mathematics
University of Texas at Austin
Microsoft Research
rward@math.utexas.edu

ABSTRACT

Numerous developments in the recent literature show the promising potential of deep learning in obtaining numerical solutions to partial differential equations (PDEs) beyond the reach of current numerical solvers. However, data-driven neural operators all suffer from the same problem: the data needed to train a network depends on classical numerical solvers such as finite difference or finite element, among others. In this paper, we propose a new approach to generating synthetic functional training data that does not require solving a PDE numerically. The way we do this is simple: we draw a large number N of independent and identically distributed ‘random functions’ u_j from the underlying solution space (e.g., $H_0^1(\Omega)$) in which we know the solution lies according to classical theory. We then plug each such random candidate solution into the equation and get a corresponding right-hand side function f_j for the equation, and consider $(f_j, u_j)_{j=1}^N$ as supervised training data for learning the underlying inverse problem $f \rightarrow u$. This ‘backwards’ approach to generating training data only requires derivative computations, in contrast to standard ‘forward’ approaches, which require a numerical PDE solver, enabling us to generate a large number of such data points quickly and efficiently. While the idea is simple, we hope that this method will expand the potential for developing neural PDE solvers that do not depend on classical numerical solvers.

Keywords Synthetic data · Numerical PDEs · Neural operators

1 Introduction

The use of deep learning for obtaining numerical solutions to PDE problems beyond the reach of classical solvers shows promise to revolutionize science and technology. Deep learning-based methods have overcome many challenges that classical numerical methods suffer from, among which are the curse of dimensionality and grid dependence.

Methods that attempt to solve PDE problems using deep learning can be split into two main classes: those that solve an instance of a PDE problem by directly approximating the solution (e.g. (6), (25), (20), (33), (32), (3)), and those that consider solutions to a family of PDE problems, also known in the literature as parametric PDEs, through operator learning. In the operator learning approach, the goal is to learn an operator that maps the known parameters to the unknown solution (e.g. (16), (2), (12), (10), (21)). In this paper, we focus on the second class, where we seek solutions to a class of PDE problems instead of an instance. Although the approach we describe is general, we focus on the Fourier Neural Operator (FNO) (10), which is a state-of-the-art neural operator learning method at the time that this paper is being written. We stress that our method is independent of the particular neural operator learning architecture and should remain applicable as a synthetic data generation plug-in as the state-of-the-art architecture evolves.

To the best of our knowledge, classical numerical methods, such as finite differences, finite element (27), pseudo-spectral methods, or other variants, have been used in order to obtain data for training purposes in operator learning. In particular, some works have used finite difference schemes (e.g. (16), (2), (13), (26), (19), (23), (21), (17)). In other works, data has been generated by constructing examples that have a closed-form explicit solution or by using schemes such as finite element, pseudo-spectral schemes, fourth-order Runge-Kutta, forward Euler, etc. (e.g. (15), (30), (8), (22), (11),

*Corresponding author

(14), (24), (28), (4), (29), (18), (31)). While these works are a strong proof-of-concept for neural operators, it is critical to move away from using classical numerical solvers to generate training data for neural operator learning if we want to develop neural operators as a general-purpose PDE solver *beyond* the reach of classical numerical solvers.

Our approach. Our approach is conceptually simple: suppose we want to train a neural network to learn solutions to a parameterized class of PDE problems of the form (1), which is a form where we know in theory that the solution for any value of the parameter belongs to a Sobolev space which has an explicit orthonormal basis of eigenfunctions and associated eigenvalues. We can generate a large number of synthetic training functions $\{u_{a_j}^k\}_{j,k}$ in the space as random linear combinations of the first M eigenfunctions, scaled by the corresponding eigenvalues. We can efficiently generate corresponding right-hand side functions $f_{a_j}^k$ by computing derivatives, $-L_{a_j}u_{a_j}^k = f_{a_j}^k$. We then use training data $(f_{a_j}^k, a_j, u_{a_j}^k)_{j=1}^N$ to train a neural operator to learn the class of PDEs.

Recall the standard supervised learning setting where the training data are input-output pairs (x_j, y_j) , where the input vectors x_j are independent and identical draws from an underlying distribution \mathcal{D} , and $y_j = \mathcal{G}(x_j)$, and the goal is to derive an approximation $\tilde{\mathcal{G}}$ with minimal test error $\mathbb{E}_{x \sim \mathcal{D}} |\tilde{\mathcal{G}}(x) - \mathcal{G}(x)|$. In our setting, the function to learn is the operator $\mathcal{G} : (a, f) \rightarrow u$. Our method of generating $(a_j, f_{a_j}^k)$ and our approach can be viewed as a best attempt within the operator learning framework to replicate training data within the classical supervised learning setting.

Organization of the paper. The order of this paper goes as follows: in Section 2 we introduce the main idea in more details, in Section 3 we discuss how to determine a space for the unknown functions depending on the problem; and in Section 4 we present some numerical experiments when using our data into known network architectures such as the Fourier Neural Operator (10) (FNO). The types of PDE problems we consider are elliptic linear and semi-linear second order equations with Dirichlet and Neumann boundary conditions, starting with the Poisson equation as a first example and then considering more complicated equations. At the end of this paper, we include an appendix section that includes a description of the mathematical symbols used in this paper. Our data generation code can be found on GitHub under the name synthetic-data-for-neural-operators.

2 Set-up and Main Approach

Consider a class of PDE problems of the form

$$\begin{cases} -L_a u = f & \text{in } \Omega \\ B(u) = 0 & \text{on } \partial\Omega, \end{cases} \quad (1)$$

where $L = L_a$ denotes a differential operator parameterized by $a \in \mathcal{A}$, $\Omega \subset \mathbb{R}^n$ is a given bounded domain, and $B(u)$ denotes a given boundary condition. The goal is to find a solution u that solves (1) given L_a and f . So in a general setting, we wish to learn an operator of the form

$$\begin{aligned} \mathcal{G} : \mathcal{A} \times \mathcal{F} &\longrightarrow \mathcal{U} \\ (a, f) &\longmapsto u, \end{aligned}$$

where \mathcal{A} , \mathcal{F} and \mathcal{U} are function spaces that depend on the specific PDE problem. For example, if we take $Lu = \Delta u$, and $B(u) = u$ then (1) becomes the Poisson equation with zero Dirichlet boundary condition. In that case, we can take $\mathcal{F} = L^2(\Omega)$ and $\mathcal{U} = H_0^1(\Omega)$ and the operator we wish to learn is of the form

$$\begin{aligned} \mathcal{G} : L^2(\Omega) &\longrightarrow H_0^1(\Omega) \\ f &\longmapsto u, \end{aligned}$$

So instead of first fixing a function f then solving (1) to obtain u to be used as input-output pairs (f, u) , we instead generate u first, plug it into (1), and compute f by the specified rule.

The main innovation of our work is in determining the appropriate class of functions for the unknown function u in (1). While from the PDE theory we know that u lives in some Sobolev space (see e.g (7)) in the case of elliptic PDEs, such spaces are infinite-dimensional, and it is unclear at first how to generate functions that serve as good representatives of the full infinite-dimensional space. We propose to generate functions as random linear combinations of basis functions of the corresponding Sobolev space. In the case where we know from theory that the underlying Sobolev space is $H_0^1(\Omega)$ or $H^1(\Omega)$, then we can obtain explicit basis elements that are given by the eigenfunctions of the Laplace operator with Dirichlet and Neumann boundary conditions, respectively.

3 Drawing synthetic representative functions from a Sobolev space

Let $\Omega \subset \mathbb{R}^n$ be a bounded and smooth domain, then the eigenvalue problem for the Laplace operator with zero Dirichlet or Neumann boundary value condition is given by

$$\begin{cases} -\Delta u = \lambda u & \text{in } \Omega \\ B(u) = 0 & \text{on } \partial\Omega, \end{cases} \quad (2)$$

where B denotes the boundary condition. Here, we consider the two cases of Dirichlet and Neumann boundary conditions, which are given by $B(u) = u$ and $B(u) = \nabla u \cdot \nu$, respectively, where ν denotes the exterior normal derivative of $\partial\Omega$. From theory, we have that in each of the two cases for B , the problem (2) has countably many (nonnegative) eigenvalues, and the corresponding eigenfunctions form an orthonormal basis for $L^2(\Omega)$. We reference chapter 8 of (1) on the details of the spectral analysis of the Laplacian.

Let $\{\varphi_n\}_{n=1}^\infty$ denote the eigenfunctions of problem (2), and let $\{\lambda_n\}_{n=1}^\infty$ denote the corresponding eigenvalues for the Dirichlet case, $B(u) = u$. Let $\{\psi_n\}_{n=1}^\infty$ be the eigenfunctions of the problem (2) and $\{\mu_n\}_{n=1}^\infty$ the corresponding eigenvalues for the Neumann case, $B(u) = \nabla u \cdot \nu$. For the Dirichlet case, the normalized family of the eigenfunctions $\varphi_n/\sqrt{\lambda_n}$ forms an orthonormal basis for $H_0^1(\Omega)$ equipped with the scalar product $\langle u, v \rangle = \int_\Omega \nabla u \cdot \nabla v$. For the Neumann case, if we define $V = \{u \in H^1(\Omega) : \int_\Omega u = 0\}$ (which is also a Hilbert space with the same scalar product as $H^1(\Omega)$), then the normalized family of the eigenfunctions $\psi_n/\sqrt{\mu_n}$ forms an orthonormal basis for V .

3.1 Representative functions in square domains

For the square domain $\Omega = (0, 1)^2$, sequences of eigenvalues and eigenfunctions of the problem (2) are known explicitly. Namely, for the Dirichlet case, eigenfunctions and the corresponding eigenvalues are given by

$$\varphi_{ij} = \sin(i\pi x) \sin(j\pi y), \quad \lambda_{ij} = (i\pi)^2 + (j\pi)^2 \quad (3)$$

and in the Neumann case, they are given by

$$\psi_{ij} = \cos(i\pi x) \cos(j\pi y), \quad \mu_{ij} = (i\pi)^2 + (j\pi)^2 \quad (4)$$

Further normalizing the eigenfunctions, we set

$$u_{ij} := \frac{\sin(i\pi x) \sin(j\pi y)}{\sqrt{\lambda_{ij}}}, \quad v_{ij} := \frac{\cos(i\pi x) \cos(j\pi y)}{\sqrt{\mu_{ij}}} \quad (5)$$

which serve as orthonormal basis elements for $H_0^1(\Omega)$ and V , respectively.

Finally, we now generate our function u by considering linear combinations of the above basis functions in (5) (that is, we consider a truncation up to some positive number M instead of considering the whole series). We use the u_{ij} 's when considering elliptic problems with zero Dirichlet boundary condition, and we use the v_{ij} for with zero Neumann condition. Namely, let $a_{ij} \sim N(0, 1/(i+j))$ and $M \in \mathbb{N}$, and set

$$u(x, y) = \sum_{i,j=1}^M a_{ij} u_{ij}, \quad v(x, y) = \sum_{i,j=1}^M a_{ij} v_{ij} \quad (6)$$

Notice that by construction, functions of the form (6) satisfy the zero Dirichlet and zero Neumann boundary conditions, respectively. In figure 1 we show representative functions of the form (6) when $M = 5$ and $M = 20$ and notice that for larger M , we have larger oscillations as opposed to smaller M .

Remark 1. *The above discussion pertains to the case when Ω is a square domain in \mathbb{R}^2 . Eigenvalues and eigenfunctions of the Laplacian have been studied (e.g. (9)) for domains that are non-square and/or in higher dimensions, suggesting that our approach can be extended to more general domains Ω . In this paper, we restrict to experiments for the case where Ω is the unit square in \mathbb{R}^2 for simplicity.*

4 Numerical Experiments using the Fourier Neural Operator

The architecture we use for numerical experiments is the Fourier Neural Operator (FNO) introduced in (10), which is able to learn mappings between function spaces of infinite dimensions. The advantage of FNO is that it aims to approximate an operator that learns to solve a family of PDEs by mapping known parameters to the solution of that

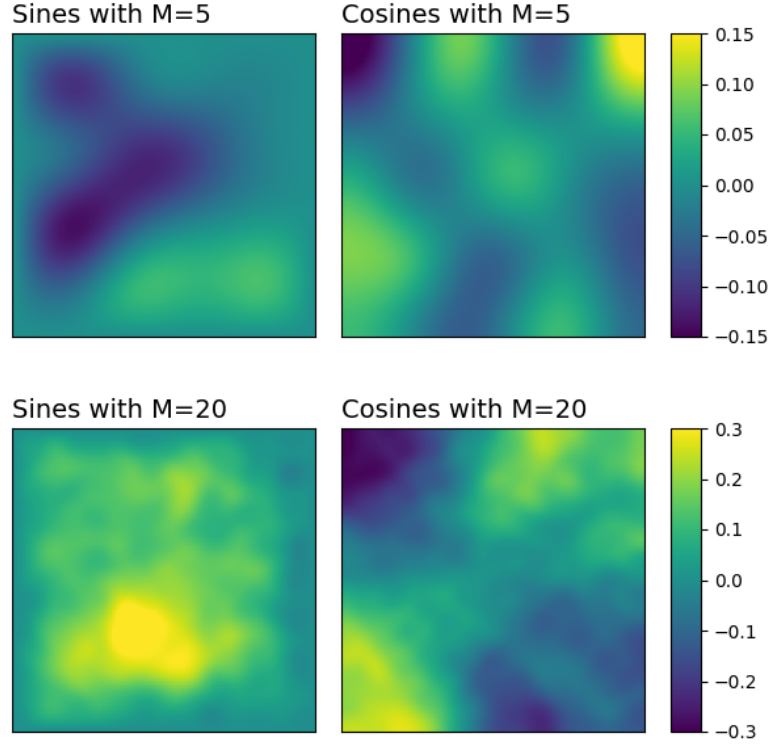


Figure 1: Example plots of functions of the form (6) for $M = 5$ and $M = 20$.

PDE, instead of only approximating one instance of a PDE problem. Due to the nature of FNO, this enables us to use our synthetic data in order to approximate an entire class of problems at once. The novelty of FNO is that the kernel function, which is learned from the data, is parameterized directly in Fourier space, leveraging the Fast Fourier Transform when computing the kernel function. We train FNO using Adam optimizer on batches of size 100, with learning rate of 0.001, modes set to 12 and of width 64. We also use relative L_2 error to measure performance for both training and testing.

We focus on second order semi-linear elliptic PDE equations in divergence form defined on $\Omega := (0, 1)^2$, with zero boundary conditions, given by

$$\begin{cases} -\operatorname{div}(A(x) \cdot \nabla u) + c(u) = f & \text{in } \Omega \\ B(u) = 0 & \text{on } \partial\Omega, \end{cases} \quad (7)$$

where $A(x) \in \mathbb{R}^{2 \times 2}$, $c(u)$ is some nonlinear function in u and $B(u)$ is either $B(u) = u$ or $B(u) = \nabla u \cdot \nu$, where ν is the exterior unit normal vector to the boundary $\partial\Omega$ that correspond to zero Dirichlet or Neumann condition, respectively. Here we also assume that A is uniformly elliptic and each $a_{ij} \in L^\infty(\Omega)$ with $i, j \in \{1, 2\}$. Note that, as a special case, for $A = I$ and $c(u) \equiv 0$, (7) reduces to the Poisson equation.

For the rest of the paper, we will denote by $H(\Omega)$ the corresponding Sobolev space depending on $B(u)$, which is $H(\Omega) = H_0^1(\Omega)$ when $B(u) = u$ and $H(\Omega) = H^1(\Omega)$ when $B(u) = \nabla u \cdot \nu$.

4.1 The Poisson Equation

First, we consider the simple example of problem (7), the Poisson equation

$$\begin{cases} -\Delta u = f & \text{in } \Omega \\ B(u) = 0 & \text{on } \partial\Omega, \end{cases} \quad (8)$$

Our goal is to learn an operator of the form:

$$G^\dagger : L^2(\Omega) \longrightarrow H(\Omega)$$

$$f \longmapsto u$$

We now generate data points of the form (f, u) where u is defined as in (6) depending on $B(u)$, and f is computed by taking derivatives of u so that (8) holds. This way, we can generate a lot of data. Notice that the Poisson equation can be easily solved when fixing f , however, here we would like to demonstrate the method of generating data through the proposed method. As we will see later, obtaining solutions to the more general problem (7) is much more difficult, and in order to obtain data for neural operators, until now, classical numerical solvers have been used.

For the Poisson equation, we generate data points as described above and let M in (6) range between 1 and 20, so that we can get a variety of such functions and various oscillations. We perform experiments by training with 1,000, 10,000 and 100,000 functional data points and testing with 100 data points for the Poisson problem with Dirichlet and then with Neumann boundary conditions. We report the relative L_2 errors in the following table 1.

	Dirichlet			Neumann		
Training points	1,000	10,000	100,000	1,000	10,000	100,000
Training loss	0.02114	0.00413	0.00109	0.01431	0.00359	0.00123
Testing loss	0.05429	0.00533	0.00117	0.03341	0.00518	0.00127

Table 1: FNO performance on the Poisson equation using our synthetic data generated as in (6).

Testing on f beyond finite trigonometric sums. Notice that if u is represented as a finite linear sum of sines and cosines, as in (6), then f generated according to (8) also consists of a finite linear sum of sines or cosines depending on B . Restricting our attention to the Dirichlet case, let us generate f so that it does not consist of sine or cosine functions. This is akin to out-of-distribution testing in the machine learning literature. We consider the following two example functions: $f(x, y) = x - y$, which is smooth, and $f(x, y) = |x - 0.5||y - 0.5|$, which has corners and is not everywhere differentiable in Ω . However, in each case, f is in $L^2(\Omega)$, and approximation of L^2 functions by trigonometric functions is well studied, and error bounds are available (see (5)). So we expect to obtain approximate solutions to the Poisson equation (8) for any f function that is in $L^2(\Omega)$.

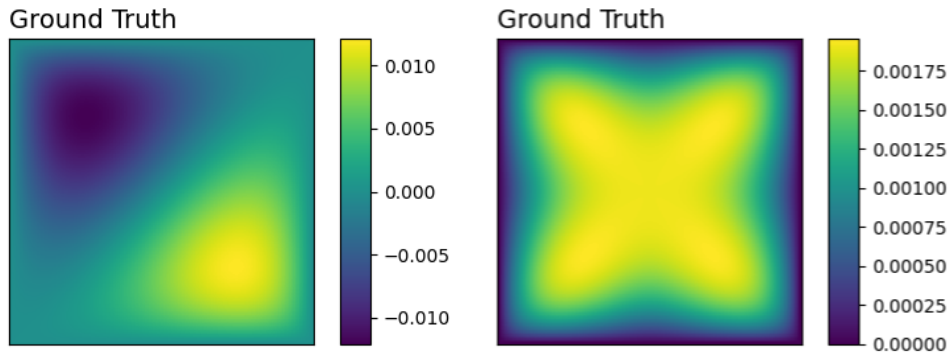


Figure 2: Ground truth of the Poisson equation when $f(x, y) = x - y$ (left) and $f(x, y) = |x - 0.5||y - 0.5|$ (right)

In Figure 3, we summarize the predicted solutions using FNO, when trained with 1,000, 10,000 and 100,000 synthetic data functions that consist of sine functions given by (6). The following demonstrates that the choice of functions u defined as in (6) generalizes well.

Note that FNO performs better when predicting a solution to the Poisson equation when the right-hand side is given by a smooth function and has a harder time when the right-hand side has corners and is not everywhere differentiable in Ω .

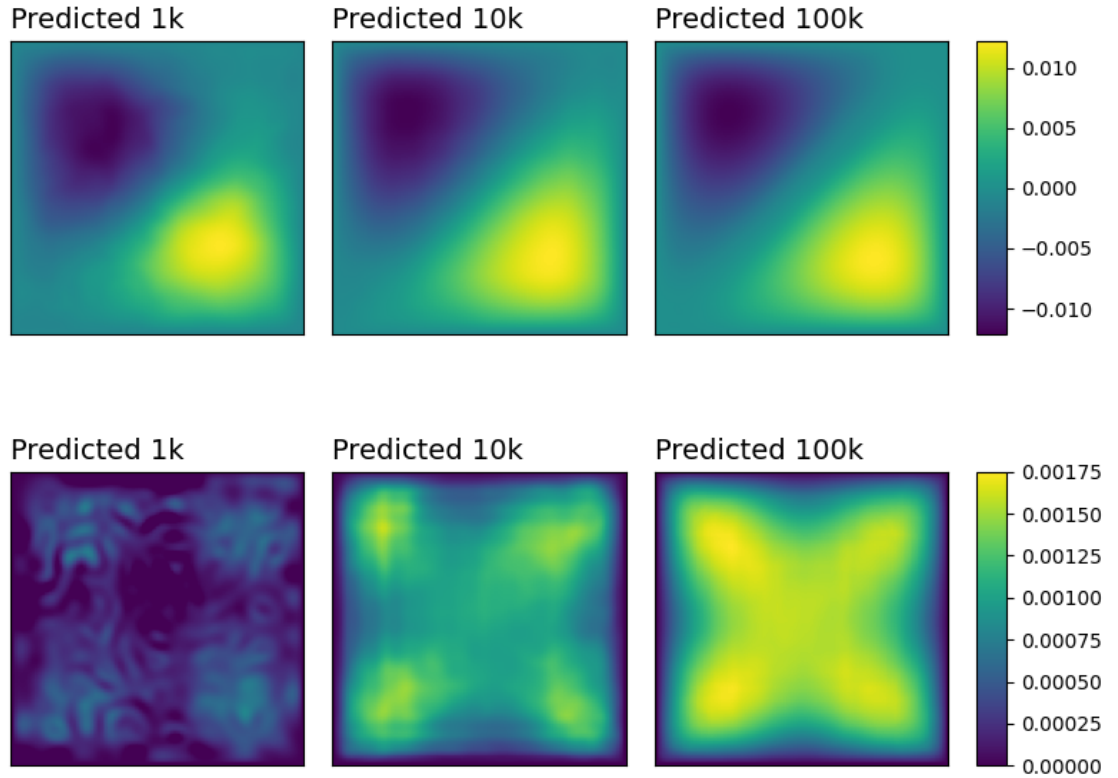


Figure 3: Predicted solutions using FNO when trained with 1, 000, 10, 000 and 100, 000 functional data points

4.2 Second order linear elliptic PDE

In problem (7), take $c(u) = 0$ and allow the matrix A to be of any form, possibly depending on (x, y) . Then (7) becomes

$$\begin{cases} -\operatorname{div}(A \cdot \nabla u) = f & \text{in } \Omega \\ B(u) = 0 & \text{on } \partial\Omega, \end{cases} \quad (9)$$

In general, since we use derivatives in our computations, we assume that the entries of A are once differentiable in the corresponding variables.

A as a fixed matrix. First, we look at the case where we fix a matrix A . Then we compute the derivatives involved for the components of A and save those as well. We generate a function u according to (6), plug it in to (9), and then compute f . As before, the goal is to learn the operator

$$\begin{aligned} G^\dagger : L^2(\Omega) &\longrightarrow H^1(\Omega) \\ f &\longmapsto u \end{aligned}$$

For a numerical experiment, let A be as follows

$$A = \begin{pmatrix} x^2 & \sin(xy) \\ x + y & y \end{pmatrix} \quad (10)$$

In this case, FNO is learning a family of solutions for a fixed A defined above of the problem (9) for varying pairs of f and u functions. This choice of A is not particularly special, and the same process can be repeated for any positive definite A (so that (9) is elliptic). For the most accurate results, we can re-generate data points of the form (f, u) for each new matrix A and train different A -dependent neural networks. The following table 2 summarizes the relative L_2 errors when using FNO to solve (9) when A is given by (10) and when training with 1, 000, 10, 000 and 100, 000 data points and testing with 100 data points.

	Dirichlet			Neumann		
Training points	1,000	10,000	100,000	1,000	10,000	100,000
Training loss	0.03545	0.00853	0.00319	0.03383	0.00840	0.00152
Testing loss	0.06309	0.01013	0.00333	0.09046	0.01146	0.00147

 Table 2: FNO performance on the problem (9) with A given by (10), using (6) functions.

A as a parametric matrix. As a more general-purpose approach to solving elliptic PDEs using FNO and synthetic data, we can also attempt to train a single neural network for an entire parameterized family of matrices A , by passing A as an input in the training data pair. That is, instead of fixing the matrix A in our synthetic data, we vary A within a parameterized class and pass it as input data together with f . In other words, the learning operator is of the form $G^\dagger : (f, A) \mapsto u$. For simplicity, we assume here that A is a diagonal matrix of the form

$$A(x, y) = \begin{pmatrix} \alpha(x, y) & 0 \\ 0 & \delta(x, y) \end{pmatrix}$$

Here, we vary $\alpha(x, y)$ and $\delta(x, y)$. In other words, the operator we are trying to learn is given by

$$G^\dagger : L^2(\Omega) \times L^\infty(\Omega) \times L^\infty(\Omega) \longrightarrow H(\Omega) \\ (f, \alpha, \delta) \mapsto u$$

To further simplify, we assume the components of A are linear functions in x, y , that is

$$A(x, y) = \begin{pmatrix} m_1x + m_2y & 0 \\ 0 & m_3x + m_4y \end{pmatrix}$$

where m_i 's uniformly distributed in $[0.1, 5]$ and u is generated according to (6) with $M \in \{1, 2, \dots, 10\}$. For each generated data point, we generate a matrix of the above form and a function u according to (6), then plug them both in equation (9) to compute f . Finally, the input data forms a triple (f, α, δ) , while the target is to predict u . This way, FNO learns how to solve a *family* of functions satisfying (9). We summarize the relative L_2 errors in table 3 using FNO when training with 1,000, 5,000 and 10,000 data points. As we can see below and as expected, the performance of the FNO with more degrees of freedom in the input data is worse compared to the case where the matrix A is considered fixed and held constant across all the input data.

	Dirichlet			Neumann		
Training points	1,000	5,000	10,000	1,000	5,000	10,000
Training loss	0.12266	0.07352	0.03134	0.14295	0.04639	0.01107
Testing loss	0.27257	0.10641	0.04885	0.25906	0.07611	0.05508

 Table 3: FNO performance on the problem (9) with varying matrix A , using (6) functions.

4.3 Second order semi-linear elliptic PDE

As a final experiment, we consider again (7) with $A = I$ and $c(u) = e^{2u}$. In this case, the problem becomes

$$\begin{cases} -\Delta u + e^{2u} = f & \text{in } \Omega \\ B(u) = 0 & \text{on } \partial\Omega, \end{cases} \quad (11)$$

As before, we generate u as specified in (6) and compute f by plugging into (11). Notice that we now have a non-linear term in u . However, from the theory, we know that the space of solutions is still $H(\Omega)$. Numerical experiments show that despite the non-linearity in that term, we see that FNO achieves low L_2 relative errors, as indicated in table 4. We summarize the relative L_2 errors of training and testing loss in table 4 when we train on 1,000, 10,000 and 100,000 data points and test on 100 data points.



Figure 4: Relative L_2 errors with standard errors, over 10 experiments with fixed diagonal matrices linear in x and y .

	Dirichlet			Neumann		
Training points	1,000	10,000	100,000	1,000	10,000	100,000
Training loss	0.02310	0.00977	0.00372	0.01139	0.00432	0.00198
Testing loss	0.03141	0.00994	0.00352	0.03141	0.00996	0.00351

Table 4: FNO performance on the problem (11) using (6) functions.

5 Conclusion and future work

Using deep learning to solve PDEs has been very promising in recent years. Here, we propose a method that eliminates the need to repeatedly solve a PDE for obtaining training data used in neural operators by first generating the unknown solution and then computing the right-hand side of the equation. Although we exclusively provide theoretical motivation and numerical experiments for second-order elliptic PDEs, this concept can be extended to other types of PDEs where the solution space is known beforehand, enabling the construction of representative functions for such solution spaces. This method could open up the possibility of obtaining good predictions for PDE problems using data-driven neural operators, for which the training data does not require classical numerical solvers to generate. We stress that our synthetic data generation approach is computationally efficient, particularly compared to solving new PDE problems numerically to generate training data for each new problem instance. We believe that our approach is important towards reaching the ultimate goal of *using deep learning to solve PDEs that are outside the scope of what we can solve using classical numerical solvers*. We note that as a by product, our method eliminates sources of error coming from numerically solving PDE problems; instead, our synthetic training data is of the form of exact solutions to a problem on a fixed-size grid.

Acknowledgments

EH and RW were supported in part by AFOSR MURI FA9550-19-1-0005, NSF DMS-1952735, NSF IFML grant 2019844, NSF DMS-N2109155, and NSF 2217033 and NSF 2217069.

References

- [1] H. Attouch, G. Buttazzo, and G. Michaille. *Variational Analysis in Sobolev and BV Spaces: Applications to PDEs and Optimization, Second Edition*. MOS-SIAM Series on Optimization. Society for Industrial and Applied Mathematics, 2014.
- [2] K. Bhattacharya, B. Hosseini, N. B. Kovachki, and A. M. Stuart. Model reduction and neural networks for parametric pdes. *CoRR*, abs/2005.03180, 2020.
- [3] O. Bilgin, T. Vergutz, and S. Mehrkanoon. GCN-FFNN: A two-stream deep model for learning solution to partial differential equations. *Neurocomputing*, 511:131–141, 2022.

- [4] Q. Cao, S. Goswami, and G. E. Karniadakis. LNO: laplace neural operator for solving differential equations. *CoRR*, abs/2303.10528, 2023.
- [5] R. A. DeVore and G. G. Lorentz. *Constructive approximation*, volume 303. Springer Science & Business Media, 1993.
- [6] W. E and B. Yu. The deep ritz method: A deep learning-based numerical algorithm for solving variational problems. *CoRR*, abs/1710.00211, 2017.
- [7] L. Evans. *Partial Differential Equations*. Graduate studies in mathematics. American Mathematical Society, 2010.
- [8] V. Fanaskov and I. V. Oseledets. Spectral neural operators. *CoRR*, abs/2205.10573, 2022.
- [9] D. S. Grebenkov and B.-T. Nguyen. Geometrical structure of laplacian eigenfunctions. *SIAM Review*, 55(4):601–667, 2013.
- [10] N. B. Kovachki, Z. Li, B. Liu, K. Azizzadenesheli, K. Bhattacharya, A. M. Stuart, and A. Anandkumar. Neural operator: Learning maps between function spaces. *CoRR*, abs/2108.08481, 2021.
- [11] Z. Li, D. Z. Huang, B. Liu, and A. Anandkumar. Fourier neural operator with learned deformations for pdes on general geometries. *CoRR*, abs/2207.05209, 2022.
- [12] Z. Li, N. B. Kovachki, K. Azizzadenesheli, B. Liu, K. Bhattacharya, A. M. Stuart, and A. Anandkumar. Neural operator: Graph kernel network for partial differential equations. *CoRR*, abs/2003.03485, 2020.
- [13] Z. Li, N. B. Kovachki, K. Azizzadenesheli, B. Liu, A. M. Stuart, K. Bhattacharya, and A. Anandkumar. Multipole graph neural operator for parametric partial differential equations. In H. Larochelle, M. Ranzato, R. Hadsell, M. Balcan, and H. Lin, editors, *Advances in Neural Information Processing Systems 33: Annual Conference on Neural Information Processing Systems 2020, NeurIPS 2020, December 6-12, 2020, virtual*, 2020.
- [14] H. Lin, L. Wu, Y. Xu, Y. Huang, S. Li, G. Zhao, and S. Z. Li. Non-equispaced fourier neural solvers for pdes. *CoRR*, abs/2212.04689, 2022.
- [15] Z. Long, Y. Lu, X. Ma, and B. Dong. Pde-net: Learning pdes from data. In J. G. Dy and A. Krause, editors, *Proceedings of the 35th International Conference on Machine Learning, ICML 2018, Stockholmsmässan, Stockholm, Sweden, July 10-15, 2018*, volume 80 of *Proceedings of Machine Learning Research*, pages 3214–3222. PMLR, 2018.
- [16] L. Lu, P. Jin, and G. E. Karniadakis. Deeponet: Learning nonlinear operators for identifying differential equations based on the universal approximation theorem of operators. *CoRR*, abs/1910.03193, 2019.
- [17] R. Molinaro, Y. Yang, B. Engquist, and S. Mishra. Neural inverse operators for solving PDE inverse problems. In A. Krause, E. Brunskill, K. Cho, B. Engelhardt, S. Sabato, and J. Scarlett, editors, *International Conference on Machine Learning, ICML 2023, 23-29 July 2023, Honolulu, Hawaii, USA*, volume 202 of *Proceedings of Machine Learning Research*, pages 25105–25139. PMLR, 2023.
- [18] F. Pichi, B. Moya, and J. S. Hesthaven. A graph convolutional autoencoder approach to model order reduction for parametrized pdes. *CoRR*, abs/2305.08573, 2023.
- [19] M. A. Rahman, Z. E. Ross, and K. Azizzadenesheli. U-NO: u-shaped neural operators. *CoRR*, abs/2204.11127, 2022.
- [20] M. Raissi, P. Perdikaris, and G. E. Karniadakis. Physics-informed neural networks: A deep learning framework for solving forward and inverse problems involving nonlinear partial differential equations. *J. Comput. Phys.*, 378:686–707, 2019.
- [21] B. Raonić, R. Molinaro, T. D. Ryck, T. Rohner, F. Bartolucci, R. Alaifari, S. Mishra, and E. de Bézenac. Convolutional neural operators for robust and accurate learning of pdes, 2023.
- [22] J. H. Seidman, G. Kissas, P. Perdikaris, and G. J. Pappas. NOMAD: nonlinear manifold decoders for operator learning. In *NeurIPS*, 2022.
- [23] W. Shi, X. Huang, X. Gao, X. Wei, J. Zhang, J. Bian, M. Yang, and T. Liu. Lordnet: Learning to solve parametric partial differential equations without simulated data. *CoRR*, abs/2206.09418, 2022.
- [24] J. Shin, J. Y. Lee, and H. J. Hwang. Pseudo-differential integral operator for learning solution operators of partial differential equations. *CoRR*, abs/2201.11967, 2022.
- [25] J. A. Sirignano and K. Spiliopoulos. DGM: A deep learning algorithm for solving partial differential equations. *J. Comput. Phys.*, 375:1339–1364, 2018.
- [26] L. Tan and L. Chen. Enhanced deeponet for modeling partial differential operators considering multiple input functions. *CoRR*, abs/2202.08942, 2022.

- [27] V. Thomée. From finite differences to finite elements: A short history of numerical analysis of partial differential equations. *Journal of Computational and Applied Mathematics*, 128(1):1–54, 2001. Numerical Analysis 2000. Vol. VII: Partial Differential Equations.
- [28] A. Tran, A. P. Mathews, L. Xie, and C. S. Ong. Factorized fourier neural operators. In *The Eleventh International Conference on Learning Representations, ICLR 2023, Kigali, Rwanda, May 1-5, 2023*. OpenReview.net, 2023.
- [29] A. Vadeboncoeur, I. Kazlauskaite, Y. Papandreou, F. Cirak, M. Girolami, and Ö. D. Akyildiz. Random grid neural processes for parametric partial differential equations. In A. Krause, E. Brunskill, K. Cho, B. Engelhardt, S. Sabato, and J. Scarlett, editors, *International Conference on Machine Learning, ICML 2023, 23-29 July 2023, Honolulu, Hawaii, USA*, volume 202 of *Proceedings of Machine Learning Research*, pages 34759–34778. PMLR, 2023.
- [30] S. Wang, H. Wang, and P. Perdikaris. Learning the solution operator of parametric partial differential equations with physics-informed deepnets. *CoRR*, abs/2103.10974, 2021.
- [31] C. White, R. Tu, J. Kossaifi, G. Pekhimenko, K. Azizzadenesheli, and A. Anandkumar. Speeding up fourier neural operators via mixed precision. *CoRR*, abs/2307.15034, 2023.
- [32] L. Zhang, T. Luo, Y. Zhang, W. E, Z.-Q. John Xu, and Z. Ma. Mod-net: A machine learning approach via model-operator-data network for solving pdes. *Communications in Computational Physics*, 32(2):299–335, June 2022.
- [33] X. Zhang and K. C. Garikipati. Bayesian neural networks for weak solution of pdes with uncertainty quantification. *CoRR*, abs/2101.04879, 2021.

6 Appendix

List of notations and their descriptions used in this paper

Function Spaces	
$L^2(\Omega)$	space of Lebesgue-measurable functions $u : \Omega \rightarrow \mathbb{R}$ with finite norm $\ u\ _{L^2} = (\int_{\Omega} u ^2 dx)^{1/2}$.
$L^\infty(\Omega)$	space of Lebesgue-measurable functions $u : \Omega \rightarrow \mathbb{R}$ that are essentially bounded.
$H^1(\Omega)$	Sobolev space of functions $u \in L^2(\Omega)$ with $ \nabla u \in L^2(\Omega)$, equipped with the inner product $\langle u, v \rangle = \int_{\Omega} uv + \int_{\Omega} \nabla u \nabla v$ and induced norm $\ u\ _{H^1} = \ u\ _{L^2} + \ \nabla u\ _{L^2}$.
$H_0^1(\Omega)$	completion of $C_c^\infty(\Omega)$ in the norm $\ u\ _{H^1}$. If Ω is bounded, we have the equivalent norm given by $\ u\ _{H^1} = \ \nabla u\ _{L^2}$.
$C_c^\infty(\Omega)$	space of smooth functions $u : \Omega \rightarrow \mathbb{R}$ that have compact support in Ω .